

Supporting Information for:

**Restraints on backbone conformations in solid state NMR studies of uniformly labeled proteins from quantitative amide  $^{15}\text{N}$ - $^{15}\text{N}$  and carbonyl  $^{13}\text{C}$ - $^{13}\text{C}$  dipolar recoupling data**

Kan-Nian Hu<sup>a</sup>, Wei Qiang<sup>a</sup>, Guillermo A. Bermejo<sup>b</sup>, Charles D. Schwieters<sup>b</sup>, and Robert Tycko<sup>a</sup>

<sup>a</sup>Laboratory of Chemical Physics, National Institute of Diabetes and Digestive and Kidney Diseases, National Institutes of Health, Bethesda, MD 20892-0520

<sup>b</sup>Division of Computational Bioscience, Center for Information Technology, National Institutes of Health, Bethesda, MD 20892-5624

Figures S1 and S2; Tables S1 and S2

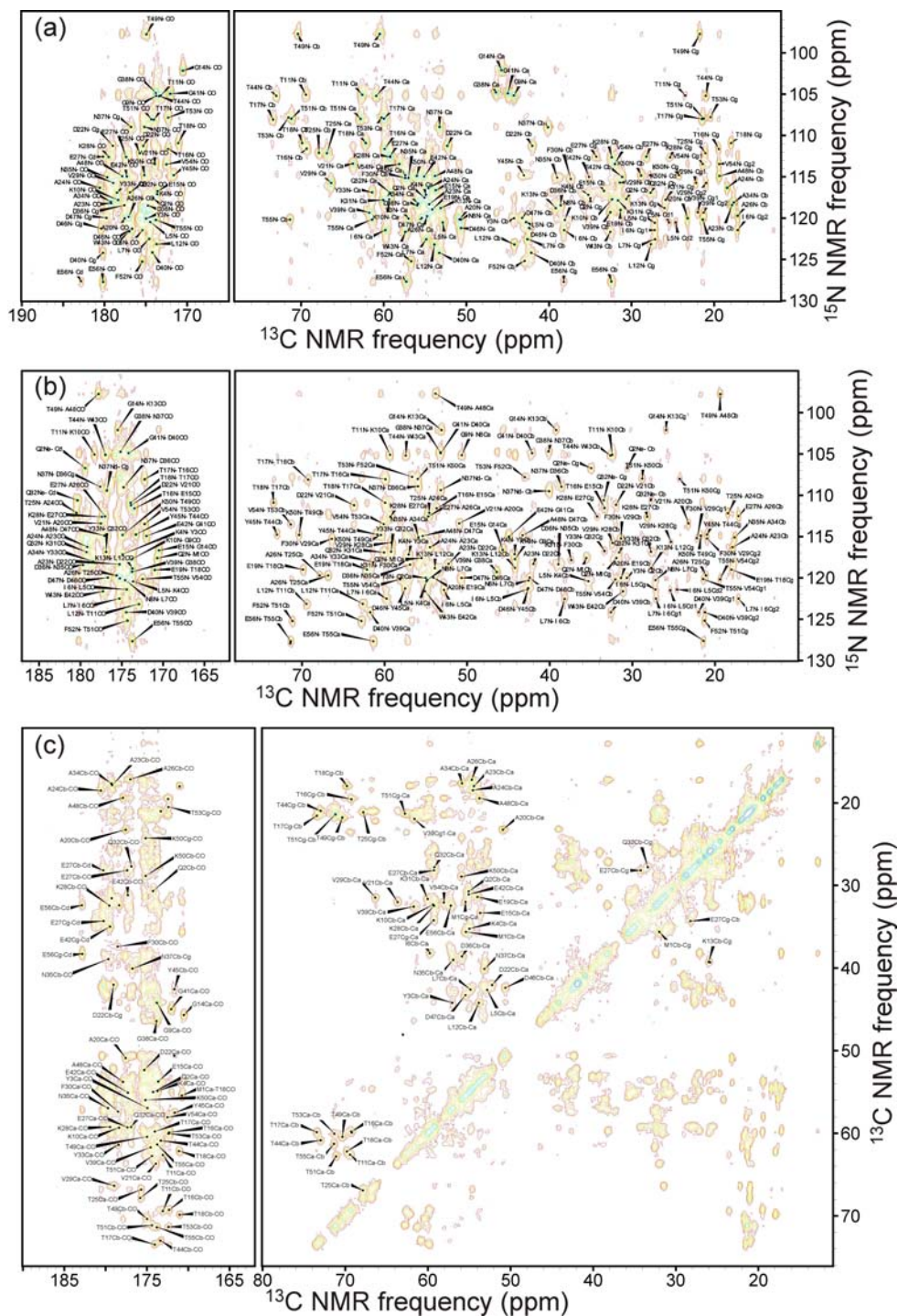


Figure S1: 2D NCACX (a), NCOCX (b), and CC (c) correlation spectra of microcrystalline, uniformly  $^{15}\text{N}$ ,  $^{13}\text{C}$ -labeled GB1, recorded at 17.6 T with MAS at 17.00 kHz. Assignments were obtained from these spectra using the MCASSIGN2 program [Hu *et al.*, J Biomolec. NMR **50**, 267-276 (2011)]. Assignments are listed in Table S1.

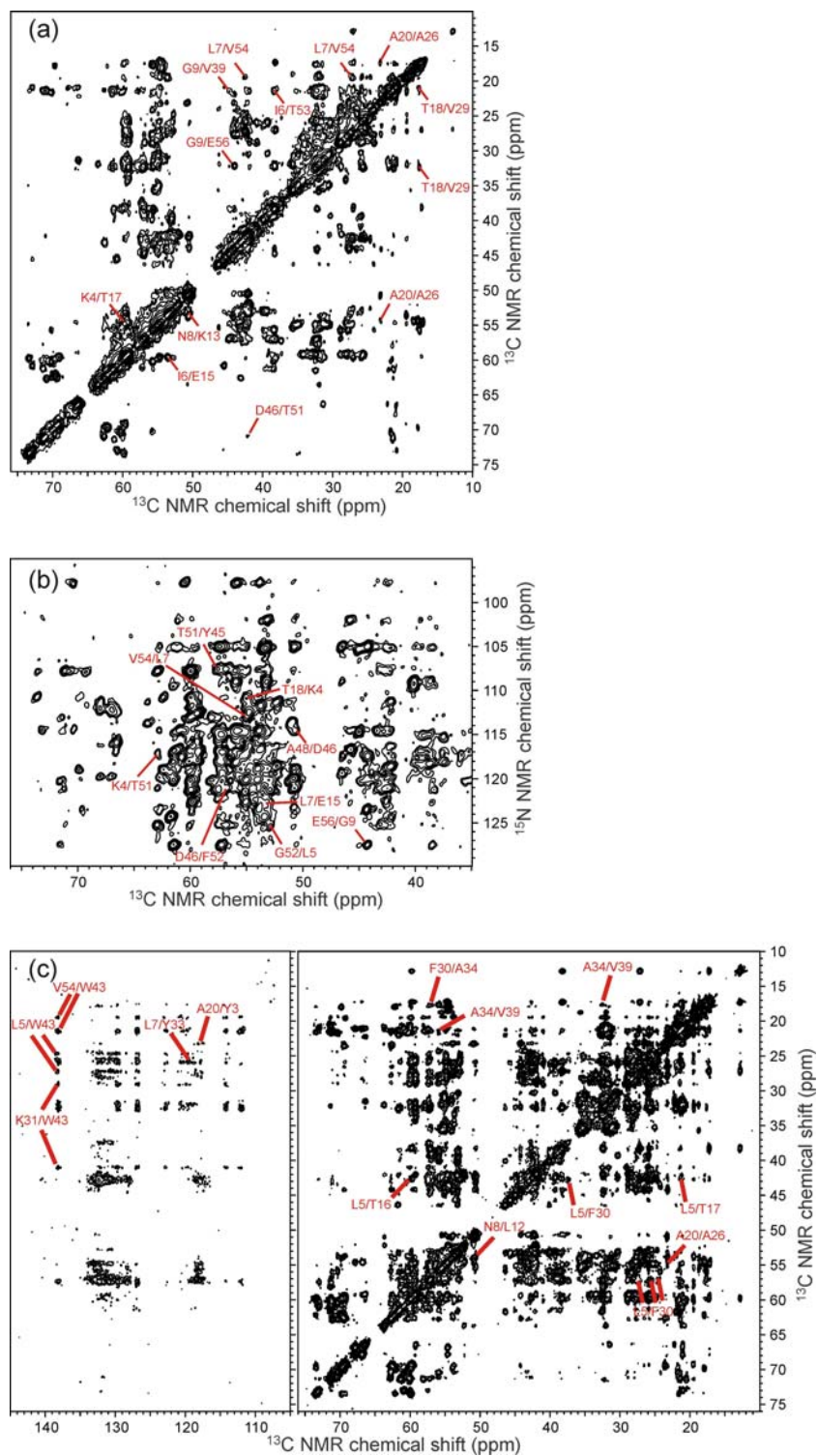


Figure S2: 2D CHHC (a), NHHC (b), and RAD (c) spectra of GB1, from which inter-residue distance restraints in Table S2 were obtained. These spectra were recorded at 17.6 T with MAS at 17.00 kHz.

Table S1: Site-specific chemical shift assignments and predicted backbone torsion angles for microcrystalline GB1. Assignments were generated in a semi-automated manner from spectral data in Fig. S1, using the program MCASSIGN2.  $^{13}\text{C}$  shifts are in ppm relative to DSS,  $^{15}\text{N}$  shifts are in ppm relative to liquid  $\text{NH}_3$ . Torsion angle predictions (in degrees) were generated by TALOS+. Only "good" predictions are shown. Predictions that were included in Xplor-NIH calculations are listed in bold font. Uncertainties were doubled in Xplor-NIH calculations. Torsion angles determined from atomic coordinates in PDB file 2GI9 are shown for comparison.

residue type	$^{13}\text{C}\alpha$ shift	$^{13}\text{C}\beta$ shift	$^{13}\text{C}\gamma$ shift	$^{13}\text{C}\delta$ shift	backbone $^{15}\text{N}$ shift	sidechain $^{15}\text{N}$ shift	TALOS+ $\phi$ prediction	TALOS+ $\psi$ prediction	$\phi, \psi$ in PDB 2GI9	
M1	170.7	55.5	35.6	31.9		33.5			---,152	
Q2	174.2	55.0	30.7	35.0	179.4	117.6	106.7	-135 $\pm$ 22	<b>147 <math>\pm</math> 14</b>	-94,127
Y3	174.9	57.0	44.2			120.0		<b>-130 <math>\pm</math> 16</b>	<b>157 <math>\pm</math> 13</b>	-115,152
K4	173.6	54.9	35.3			117.1		-152 $\pm$ 10	<b>150 <math>\pm</math> 9</b>	-114,146
L5	174.4	52.8	42.7	27.2	25.5, 24.6	120.5		<b>-117 <math>\pm</math> 16</b>	<b>133 <math>\pm</math> 17</b>	-122,125
I6	175.3	59.8	38.2	17.2, 27.2		121.4				-105,123
L7	174.6	54.9	42.6	27.2		122.5				-104,126
N8		50.7	38.1			120.2		<b>-117 <math>\pm</math> 28</b>	164 $\pm$ 26	-120,65
G9	173.7	44.2				105.2				-86,169
K10	178.3	59.3	32.4			117.7		-61 $\pm$ 7	-34 $\pm$ 10	-62,-40
T11	173.0	62.6	69.4	23.5		105.1		-105 $\pm$ 19	-2 $\pm$ 16	-107,-43
L12	173.7	53.9	44.2	27.7		123.2		-128 $\pm$ 35	153 $\pm$ 12	-111,125
K13	175.5	53.1	39.2	26.0		118.8		<b>-134 <math>\pm</math> 13</b>	<b>158 <math>\pm</math> 16</b>	-133,148
G14	170.5	45.7				102.1		-169 $\pm$ 28	162 $\pm$ 11	144,-153
E15	173.5	53.7	33.3			116.7		<b>-143 <math>\pm</math> 17</b>	<b>160 <math>\pm</math> 0</b>	-139,140
T16	172.3	59.9	69.3	19.5		111.6		<b>-125 <math>\pm</math> 31</b>	<b>153 <math>\pm</math> 14</b>	-139,171
T17	174.0	59.9	73.4	21.5		108.0		<b>-126 <math>\pm</math> 19</b>	<b>162 <math>\pm</math> 6</b>	-135,162
T18	171.0	62.2	69.8	18.0		110.9				-153,162
E19		54.1	31.4			119.0		<b>-135 <math>\pm</math> 23</b>	156 $\pm$ 14	-111,128
A20	177.5	50.9	23.2			120.0		-132 $\pm$ 35	167 $\pm$ 15	-150,156
V21	173.9	63.7	32.0			113.4		-84 $\pm$ 28	-20 $\pm$ 23	-67,-31
D22	175.3	52.3	42.0	179.0		111.2				-156,177
A23	179.2	54.5	17.9			118.3				-70,-39
A24	180.5	54.6	18.5			116.3		<b>-64 <math>\pm</math> 6</b>	<b>-38 <math>\pm</math> 7</b>	-61,-37
T25	175.7	66.8	67.8	21.1		112.1		<b>-67 <math>\pm</math> 9</b>	<b>-38 <math>\pm</math> 13</b>	-67,-47
A26	177.0	54.7	17.2			119.7		<b>-64 <math>\pm</math> 6</b>	<b>-40 <math>\pm</math> 14</b>	-60,-40
E27	177.4	59.3	28.2	34.3	180.2	112.5		<b>-65 <math>\pm</math> 10</b>	<b>-40 <math>\pm</math> 13</b>	-58,-43
K28	179.5	59.2	32.4	25.3		112.6		<b>-67 <math>\pm</math> 9</b>	<b>-45 <math>\pm</math> 9</b>	-62,-42
V29	178.9	66.4	31.4	21.0, 22.2		115.7		<b>-69 <math>\pm</math> 10</b>	<b>-40 <math>\pm</math> 9</b>	-63,-48
F30	178.5	57.3	37.4			115.2		<b>-69 <math>\pm</math> 9</b>	<b>-38 <math>\pm</math> 12</b>	-68,-36
K31	179.3	60.0	31.6	25.9		117.8		<b>-69 <math>\pm</math> 9</b>	<b>-38 <math>\pm</math> 11</b>	-65,-38
Q32	176.9	59.2	27.7	33.4	180.4	116.9	110.6	<b>-63 <math>\pm</math> 5</b>	<b>-45 <math>\pm</math> 4</b>	-64,-41
Y33	178.4	61.4				116.8		<b>-62 <math>\pm</math> 6</b>	<b>-44 <math>\pm</math> 7</b>	-59,-46
A34	179.3	55.9	17.6			118.1		<b>-61 <math>\pm</math> 6</b>	<b>-39 <math>\pm</math> 6</b>	-63,-46
N35	179.7	57.0	39.0			115.1		<b>-62 <math>\pm</math> 4</b>	<b>-41 <math>\pm</math> 6</b>	-60,-45
D36	174.8	55.9	38.6	177.6		118.4		<b>-66 <math>\pm</math> 9</b>	<b>-29 <math>\pm</math> 13</b>	-63,-46
N37	175.2	53.2	40.1	176.8		109.0	109.4	-91 $\pm$ 11	1 $\pm$ 14	-103,12
G38	173.8	46.4				104.8		85 $\pm$ 23	15 $\pm$ 11	86,10
V39	174.5	61.7	32.6	21.2, 22.0		119.3		-104 $\pm$ 14	126 $\pm$ 24	-97,134

D40	174.2	53.2	42.1	180.2		124.2		-107 ± 25	151 ± 34	-140,111
G41	172.0	45.0				104.9				-156,-164
E42	177.3	55.1	31.1	35.1	179.5	115.0		<b>-114 ± 25</b>	<b>140 ± 13</b>	-96,140
W43	177.0	57.4	32.6			121.6				-113,147
T44	173.3	60.9	73.0	21.0		105.2		<b>-135 ± 24</b>	<b>161 ± 14</b>	-131,159
Y45	171.6	57.5	42.7			114.8		<b>-149 ± 7</b>	<b>152 ± 14</b>	-136,130
D46	176.7	50.7	42.4	180.4		121.2				-119,104
D47	177.1	55.4	43.3	179.8		120.0		-64 ± 8	-28 ± 13	-62,-25
A48	177.9	53.8	19.4			114.9		-71 ± 16	-28 ± 14	-71,-16
T49	174.9	60.4	70.4	21.7		97.7		-108 ± 11	1 ± 21	-126,8
K50	175.2	56.0	28.9	24.3	27.8	114.8		61 ± 7	34 ± 11	53,40
T51	174.3	62.8	71.1	21.3		108.0				-123,129
F52	175.4	56.6	43.0			125.2		<b>-102 ± 20</b>	<b>152 ± 14</b>	-99,152
T53	172.3	60.1	71.4	20.5		107.8		<b>-143 ± 23</b>	<b>157 ± 13</b>	-129,149
V54	172.5	58.1	32.1	19.4, 21.4		113.5		<b>-122 ± 24</b>	<b>145 ± 14</b>	-131,131
T55	173.7	61.3	71.4	21.4		120.2		<b>-112 ± 18</b>	<b>131 ± 17</b>	-133,129
E56	180.2	57.2	32.4	38.2	182.8	127.7				-97,---

Table S2: Interatomic distance restraints derived from inter-residue crosspeaks in 2D CHHC, NHHC, and RAD spectra of microcrystalline GB1 in Fig. S2, and from  $^{15}\text{N}$ -BARE and  $^{13}\text{C}$ -BARE data for N- and C-terminal residues. (Note: If atom 1 and/or atom 2 can represent more than one site, *e.g.*, the three  $\text{H}_\beta$  sites of A20, then distance restraints for all possible combinations of atom 1 and atom 2 were included in the Xplor-NIH calculations.)

atom 1	atom 2	distance range (Å)	2D spectrum
I6 $\text{H}_\alpha$	E15 $\text{H}_\alpha$	1.8-2.8	CHHC
N8 $\text{H}_\alpha$	K13 $\text{H}_\alpha$	1.8-2.8	CHHC
K4 $\text{H}_\alpha$	T17 $\text{H}_\alpha$	1.8-2.8	CHHC
L12 $\text{H}_\delta$	N37 $\text{H}_\beta$	1.8-2.8	CHHC
T18 $\text{H}_\gamma$	V29 $\text{H}_\beta$	1.8-2.8	CHHC
T18 $\text{H}_\gamma$	V29 $\text{H}_\gamma$	1.8-2.8	CHHC
A20 $\text{H}_\beta$	A26 $\text{H}_\alpha$	1.8-2.8	CHHC
A20 $\text{H}_\beta$	A26 $\text{H}_\beta$	1.8-2.8	CHHC
G9 $\text{H}_\alpha$	V39 $\text{H}_\gamma$	1.8-2.8	CHHC
E42 $\text{H}_\beta$	T55 $\text{H}_\beta$	1.8-2.8	CHHC
D46 $\text{H}_\beta$	T51 $\text{H}_\beta$	1.8-2.8	CHHC
I6 $\text{H}_\beta$	T53 $\text{H}_\gamma$	1.8-2.8	CHHC
L7 $\text{H}_\beta$	V54 $\text{H}_\gamma$	1.8-2.8	CHHC
L7 $\text{H}_\gamma$	V54 $\text{H}_\gamma$	1.8-2.8	CHHC
G9 $\text{H}_\alpha$	E56 $\text{H}_\beta$	1.8-2.8	CHHC
K4 $\text{H}_\text{N}$	T51 $\text{H}_\alpha$	2.0-4.0	NHHC
L5 $\text{H}_\alpha$	F52 $\text{H}_\text{N}$	2.0-4.0	NHHC
L7 $\text{H}_\alpha$	E54 $\text{H}_\text{N}$	2.0-4.0	NHHC
G9 $\text{H}_\alpha$	E56 $\text{H}_\text{N}$	2.0-4.0	NHHC
L7 $\text{H}_\text{N}$	E15 $\text{H}_\alpha$	2.0-4.0	NHHC
K4 $\text{H}_\alpha$	T18 $\text{H}_\text{N}$	2.0-4.0	NHHC
D46 $\text{H}_\alpha$	A48 $\text{H}_\text{N}$	2.0-4.0	NHHC
D46 $\text{H}_\text{N}$	F52 $\text{H}_\alpha$	2.0-4.0	NHHC
Y45 $\text{H}_\alpha$	T51 $\text{H}_\text{N}$	2.0-4.0	NHHC
L5 $\text{C}_\delta$	F30 $\text{C}_\alpha$	3.0-7.0	RAD
L5 $\text{C}_\delta$	W43 $\text{C}_{\beta 2}$	3.0-7.0	RAD
L5 $\text{C}_\gamma$	F30 $\text{C}_\alpha$	3.0-7.0	RAD
L5 $\text{C}_\gamma$	W43 $\text{C}_{\beta 2}$	3.0-7.0	RAD
L7 $\text{C}_\delta$	Y33 $\text{C}_\zeta$	3.0-7.0	RAD
N8 $\text{C}_\alpha$	L12 $\text{C}_\alpha$	3.0-7.0	RAD
L5 $\text{C}_\beta$	T16 $\text{C}_\alpha$	3.0-7.0	RAD
L5 $\text{C}_\beta$	T17 $\text{C}_\gamma$	3.0-7.0	RAD
Y3 $\text{C}_\zeta$	A20 $\text{C}_\beta$	3.0-7.0	RAD
A20 $\text{C}_\beta$	A26 $\text{C}_\alpha$	3.0-7.0	RAD
L5 $\text{C}_\beta$	F30 $\text{C}_\beta$	3.0-7.0	RAD
K31 $\text{C}_\beta$	W43 $\text{C}_{\beta 2}$	3.0-7.0	RAD
K31 $\text{C}_\delta$	W43 $\text{C}_{\beta 2}$	3.0-7.0	RAD
K31 $\text{C}_\gamma$	W43 $\text{C}_{\beta 2}$	3.0-7.0	RAD
F30 $\text{C}_\alpha$	A34 $\text{C}_\beta$	3.0-7.0	RAD
A34 $\text{C}_\beta$	V39 $\text{C}_\beta$	3.0-7.0	RAD
Y45 $\text{C}_\zeta$	D47 $\text{C}_\beta$	3.0-7.0	RAD
W43 $\text{C}_{\beta 2}$	V54 $\text{C}_\gamma$	3.0-7.0	RAD
M1 N	Q2 N	3.1-3.5	$^{15}\text{N}$ -BARE
T55 N	E56 N	3.1-3.3	$^{15}\text{N}$ -BARE
M1 CO	Q2 CO	3.0-3.2	$^{13}\text{C}$ -BARE
T55 CO	E56 CO	2.9-3.1	$^{13}\text{C}$ -BARE